Aerospace Science and Technology 128 (2022) 107775

Contents lists available at ScienceDirect

Aerospace Science and Technology

www.elsevier.com/locate/aescte

Experimental validation of a three-dimensional through-flow model for high-speed compressor surge

Mauro Righi [a,*], Vassilios Pachidis [a], László Könözsy [a], Thomas Giersch [b], Sven Schrape [b]

[a] Cranfield University, Cranfield, MK430AL, United Kingdom
[b] Rolls-Royce Deutschland Ltd & Co KG, Dahlewitz, 15827 Blankenfelde-Mahlow, Germany

ARTICLE INFO

Article history:
Received 16 December 2021
Received in revised form 14 June 2022
Accepted 15 July 2022
Available online 21 July 2022
Communicated by Jérôme Morio

Keywords:
Compressor surge
Through-flow code
Post-stall modelling
Axial compressors
Experimental validation

ABSTRACT

This paper describes the validation of surge simulations produced using the low-order code ACRoSS with experimental data from a 4. 5-stage high-speed rig, representative of the front stages of a modern high-pressure compressor (HPC). ACRoSS is an unsteady, 3D through-flow code developed at Cranfield University to predict compressor performance during stall events. The experimental data was derived during the Rig250 build 6B test campaign, carried out in 2016 by the DLR Institute of Propulsion Technology. To correctly represent the surge events, the ducting of the testbed upstream and downstream of the compressor is included in the simulation.

The results from the low-order model are compared with measurements from unsteady probes for two surge events at design speed with different downstream plenum sizes. The surge frequency and pressure profiles in time are closely reproduced by the low-order model. Analysis of the unsteady pressure measurement and the acoustic waves modelled by ACRoSS indicates that the surge period is likely to be influenced by the reflection of the initial surge wave in the inlet duct.

Using the ACRoSS model, surge can be accurately reproduced both in 3D and 2D. Two-dimensional, axisymmetric simulations are shown to be sufficient for the cases investigated, and surge can be simulated with a computational cost of less than one hour per event using just 40 CPUs. This represents over an order of magnitude improvement in computational power and time required to simulate surge, compared to traditional URANS 3D CFD.

1. Introduction

The occurrence of compressor stall poses a great risk to the operation of modern aero-engines. This paper focuses on a type of stall called *deep surge*, in which the whole system operates periodically in reverse flow, as shown in Fig. 1. Four phases can be identified during the surge cycle: flow reversal, blowdown, recovery, and re-pressurisation. During the flow reversal and blowdown, the front of the engine is subjected to extreme mechanical and thermal loads. There is therefore an interest from engine manufacturers in the capability to accurately predict surge and the overpressure it causes on the compressor casing and engine cowl, to ensure integrity without over-designing and adding extra weight. More in general, the capability to model rotating stall and surge can be used to characterise the stall behaviour of a new compressor, and to enhance its recoverability and operability.

Experimental testing of surge, or compressor stall in general, is very rare on high-speed multi-stage machines representative of real engines [1–3]. Compressor stall experimental testing is extremely expensive and often limited to avoid damage to the rig [4,5]. Flow-field and performance measurements of compressor surge are particularly challenging due to the unsteady nature of the event and the difficulty of measuring flow speed during reversal. Unsteady measurements are often limited to static pressure taps on the casing, with massflow and pressure ratio being derived. While valuable knowledge can be obtained from experiments on the stall event, it remains uncertain as to how much results from compressor rigs relate to the same geometry installed in a multi-shaft engine.

High-fidelity CFD has been used to simulate stall at high-speed in multi-stage compressors. The compressor rig presented in this paper has been previously investigated using single passage high-fidelity URANS simulations, reproducing multiple surge events [6]. Three-dimensional full annulus modelling of compressor surge has been performed at Imperial College, using high-fidelity URANS simulations [7,8]. This type of CFD offers the best resolution of the phaenomenon, but the computational cost associated remains

* Corresponding author.
E-mail address: m.righi@cranfield.ac.uk (M. Righi).

https://doi.org/10.1016/j.ast.2022.107775
1270-9638/

Nomenclature

$\overline{E}, \overline{F}, \overline{G}$	Flux vectors		
$\overline{f}$	Body force vector		
f_N, f_{PL}	Turning force, pressure loss force		
K	Body force stiffness parameter		
M	Mach number		
$\dot{m}$	Massflow	kg/s	
PR	Normalised pressure rise		
P, P_0	Pressure, Total pressure	Pa	
r	Radial position	m	
$\overline{S}$	Source terms vector		
s	Blade pitch	m	
R_{CURV}	Local blade curvature radius	m	
t	Time	s	
TR	Normalise temperature rise		
$\overline{U}$	Conservative variables		
u	Flow velocity	m/s	
V_{ST}	Settling chamber volume	m^3	
x	Axial position	m	

Greek letters

α	Flow direction	rad
β	Local blade camber-line	rad
γ	Specific heat ratio	
γ	Stagger angle	rad
δ	Deviation	rad
ρ	Density	kg/m^3
θ	Circumferential position	rad
ω	Pressure loss coefficient	

Subscripts

IN	Domain inlet flow
LE	Leading edge
TE	Trailing edge
x	Axial direction
$\parallel, \perp$	Flow parallel and normal to blade camber-line

Acronyms

BC	Boundary conditions
HPC	High pressure compressor
IGV	Inlet guide vane
IPC	Intermediate pressure compressor
LE	Leading edge
RPM	Rotation per minute
TE	Trailing edge

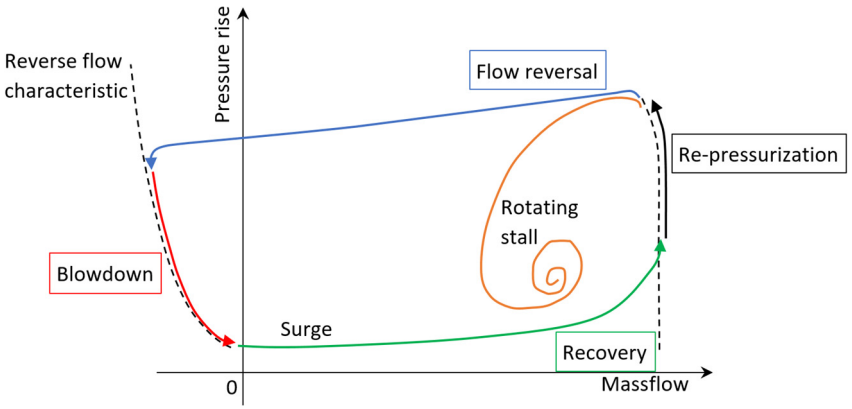

Fig. 1. Example of rotating stall and deep surge trajectories on the compressor map, with phases of surge highlighted.

in the order of a day per rotor revolution using hundreds of cores running in parallel.

To reduce the computation cost, research has focused on alternative, low-order models to simulate compressor stall. Simple 0D and 1D models [3,9] have been proposed, although these normally require some knowledge or approximation of the performance of the compressor operating in reverse and stalled flows. The 0D model proposed by Greitzer [10] famously introduced the concept of the B parameter, which describes how shaft speed and plenum size affect the compressor stall developing into a surge or a rotating stall. More complex, three-dimensional models have been proposed, with blade row performance estimated separately using empirical correlations, known as "through-flow" codes. At MIT Gong [11] and Brand [12] developed body forces for multi-stage axial compressors using 3D URANS simulation, although validation was only completed for forward flow operation and not extended to post-stall behaviour. Longley proposed a novel method to incorporate in the governing equations the effect of the flow separation inside of the blade passages, which occurs at smaller scale than what modelled by through-flow codes [13]. His code was successfully validated for rotating stall and reverse flow for low-speed 3- and 4-stage compressors. More recently, Rosa Taddei developed a 2D mean-line method for the modelling of compressor rotating stall, particularly well-suited to transonic compressors where shock occurs within the blade passages [14]. Two new three-dimensional throughflow codes have also been presented by Guo et al. [15] and Zeng et al. [16] and validated for low-speed axial compressors, demonstrating the ongoing interest in low-order stall modelling.

A three-dimensional, through-flow code has been developed at Cranfield University called ACRoSS, Axial Compressor Rotating Stall and Surge simulator. This code has been developed in the context of a study on shaft failure and turbine overspeed; since in this event the compressors are expected to stall, it was created as a tool to predict the performances in such conditions, expressed in characteristics [17].

The code has been validated for the modelling of rotating stall and surge in low-speed compressors [18] and for surge in high-speed modern compressors using data from high-fidelity URANS CFD [19]. This paper describes the validation of the surge modelling capability of ACRoSS for a high-speed compressor rig, representative of a modern aero-engine HPC. To the best of the authors' knowledge, this is the first published case of this type of experimental validation demonstrating the applicability of the method to compressors of commercial relevance. This paper also presents

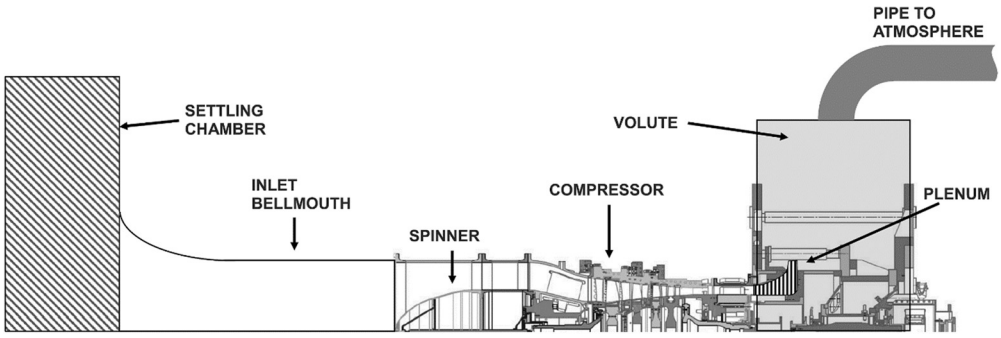

Fig. 2. The DLR Rig 250 test facility, including original image from Giersch et al. [3]. Not in scale.

some challenges which arose from the need to reproduce a compressor rig in an experimental testbed, how this influenced the numerical model set-up and how it affected the surge event itself.

2. Experimental set-up

The research rig investigated, Rig250 in Fig. 2, has 4.5 stages and its geometry is representative of a modern aero-engine HPC front block. Rig 250 is installed in the Multistage Two Shaft Compressor Test Facility (M2VP) at the DLR Institute of Propulsion Technology. The design pressure ratio is about 4.5 and the design massflow is about 46 kg/s [3]. The rig is equipped with various unsteady casing pressure measurements throughout the compressor, allowing detailed analysis of the transients during surge as well as vibration monitoring. These have been used to validate the predicted blade responses in multistage compressors [20] due to inlet distortion [21]. Further description of this rig and the M2VP test facility can be found in literature [22–26].

The rig has 3 set of variable geometries: Inlet guide vanes (IGV), stator 1 and stator 2. In the test cases analysed in this article, these were set in nominal position and did not move during the surge events.

In this test facility, the air enters the settling chamber through a nozzle positioned on the far side. Due to the pressure losses in the nozzle, the pressure in the settling chamber reduces as the massflow increases; at design speed the inlet pressure is ∼30 kPa below atmospheric. An inlet duct with a bell mouth is present in front of the compressor, about 6 times the length of the compressor.

This test facility is equipped with a variable geometry plenum downstream of the compressor. The back wall of the plenum can be moved axially to increase or reduce its volume, thus modifying the inertia of the system. In the experimental campaign considered, the plenum was set at different volumes to assess its effect on the stall. The plenum throttle exhausts in the radial direction into a volute which is connected to the atmosphere with a several meters long pipe.

The compressor is instrumented for both steady and unsteady measurements. Steady measurements include the inlet and outlet total pressure and temperature, shaft speed, massflow, and ambient pressure; additionally steady measurements of total pressure are available at each stator LE at multiple circumferential positions. Unsteady measurements of static pressure are taken using multiple sets of unsteady pressure transducers; these are positioned at the inlet of each rotor, distributed in the circumferential direction, and a probe is also present in the plenum. For the current work, the signal of the transducer is pre-processed with a low-pass filter and a constant value of ambient pressure is added to give an absolute measurement. Due to the clocking of the taps with respect to the blades and the drift in time of transducer measurement, the absolute value is not coherent between probes at the same stage or with steady measurements. Therefore, the focus in this work will be on the shape and period of the measurements during the surge cycle rather than on the absolute value. Massflow profiles during surge are not available, as this was measured at lower sample rate and with probes unsuitable for reverse flow.

The compressor is driven by electric motors and during the surge tests the rotational speed is kept constant while the operating condition is controlled by the throttle. To trigger the stall, the throttle is closed in small steps until surge is initiated. Afterwards, the throttle remains constant for several cycles before the anti-surge protection system reacts to open it again. Two surge cases at 100% corrected speed are presented in this paper, with the plenum set to its minimum and maximum volume; these are referred to hereafter as Case 1 and Case 2 respectively. In an exceptional circumstance, in the maximum volume case the stall was not triggered by throttling, but by an emergency shutdown of an electric motor which caused the compressor to rapidly decelerate.

3. Methodology

3.1. ACRoSS through-flow code

The through-flow code ACRoSS is here presented briefly, a more detailed description can be found in Righi et al. [17,18].

The low-order through-flow code used in this study solves the full 3D annulus as an empty duct and employs the body-force method to represent the effects of the blade rows. The flow is modelled using the unsteady, 3D, cylindrical Euler equations:

$$\frac{\partial}{\partial t}\left[\overline{U}\right] = -\frac{1}{r}\frac{\partial}{\partial r}\left[\overline{\mathrm{E}}\right] - \frac{1}{r}\frac{\partial}{\partial \theta}\left[\overline{\mathrm{F}}\right] - \frac{\partial}{\partial x}\left[\overline{\mathrm{G}}\right] + \overline{S} + \overline{f} \tag{1}$$

Where $\overline{U}$ is the conservative variable vector, $\overline{E}$, $\overline{F}$, $\overline{G}$ are the radial, circumferential, and axial fluxes, S is the source term vector and $\overline{f}$ is a vector formed by the body forces. Air is modelled as a thermally perfect gas. The Euler equations are solved using Godunov-style schemes, 1st order in the axial and radial directions and 2nd order in the circumferential. The whole domain is solved in the absolute frame of reference, and blade rotation is introduced using the method proposed by Gong [11].

The domain is meshed automatically creating quadrilateral volumes as in Fig. 3. Inside of the blade rows a turning and a pressure loss body-force, f_N and f_{PL}, are calculated along the pseudo-planes formed by the grid. The formulation is derived from what proposed by Longley [13] and Brand [12] and has been further developed to provide a robust algorithm suitable for high-speed transonic compressors and for the unsteady flows which occur during reversal and recovery.

$$f_{PL} = -\Delta P_0 \frac{P/P_0}{dx \cdot \cos\beta} \tag{2}$$

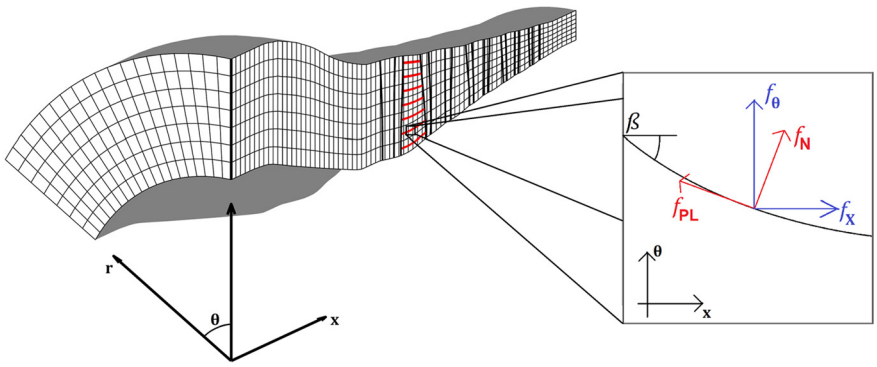

Fig. 3. Example of automatic grid generation with pseudo-planes and body force decomposition in axial and circumferential directions highlighted.

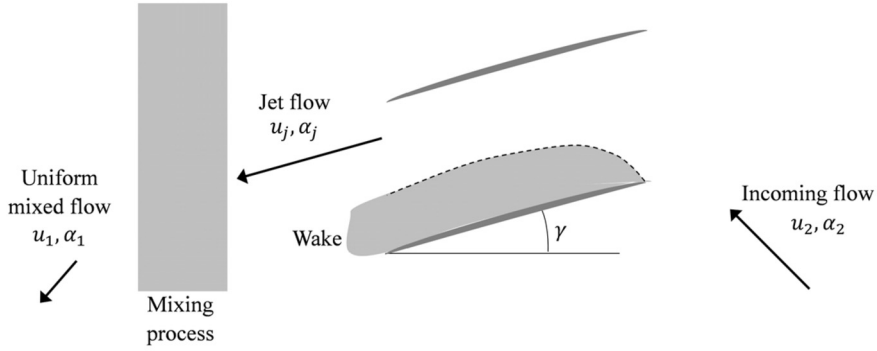

Fig. 4. Flow structure in a separated blade passage in reverse flow conditions.

$$f_N = \frac{1 - M_X^2}{\cos^2(\beta)\,(1 - M^2)} \cdot \left(\frac{\rho u_{\parallel}^2}{R_{CURV}} - \frac{\rho\,|u_x|\,u_{\perp}}{s \cos\beta} K \right) + \frac{\tan\beta (1 + (\gamma - 1) M^2)}{(1 - M^2)} f_{PL} \tag{3}$$

$$\omega = \frac{P_{0,LE} - P_{0,TE}}{P_{0,LE} - P_{LE}} \tag{4}$$

The turning body force f_N is a function of both the blade radius of curvature and the misalignment between flow and the local camber-line ($u_\perp$ is the flow normal to the local blade camber-line β). The total pressure loss along a pseudo-plane from LE to TE is calculated from the pressure loss coefficient ω using Eq. (4). The losses are then distributed between the elements inside of the blade to obtain the local total pressure loss ΔP_0, which is introduced by the loss force f_{PL} calculated using Eq. (2). The body forces are projected normal and parallel to the local flow direction to create the vector of body-forces in the x, r, θ directions.

In forward flow conditions, the blade row performance is expressed as a deviation angle δ and pressure loss coefficient ω. These are predicted using empirical correlations developed by Rolls-Royce plc and applicable to modern aero-engine core compressors. For stalled and reverse flow conditions instead, algorithms have been specifically developed from the theory proposed by Longley [13]; an example of the flow structure during reverse flow is presented in Fig. 4. In these conditions pressure losses are ignored and only the turning force f_N is used, projected normal to the blade camber-line, and not to the flow direction. The normal force turns the flow into the blade passage and, since it is directed against the incoming flow, it also introduces the pressure loss associated with the flow separation which occurs at the TE. All other loss sources (skin friction, secondary flows, tip clearances) are neglected as they are expected to be insignificant compared to the separation and wake mixing mechanism [13,27].

A deviation angle is also applied in reverse flow condition at the LE, where the flow leaves the blade passage. This is estimated based on a simplified 0D representation of the blade and is function only of the inlet flow conditions and the local blade stagger angle. A more detailed description of this method can be found in Righi et al. in [17,18].

To allow the formation of a-symmetrical structures during stall, when ACRoSS is run in 3D a random circumferential distortion is applied to the flow inside of the blade rows at constant time intervals. This distortion is quickly dissipated when the compressor is in unstalled or reverse flow conditions, while during flow reversal and recovery it can grow and create stall cells. The distortion magnitude has been calibrated through previous cases to ensure that it is strong enough to allow the creation of asymmetric structures during transients, but it does not have a significant impact on the performances measured during steady state or on the overall stall behaviour. This distortion is not introduced when the code is run in 2D.

3.2. Model setup

The code ACRoSS is used to produce a model representative of Rig250 and part of the testing facility. When generating this model, it is necessary to determine which of the components presented in Fig. 2 influences surge behaviour and should be included in the model, and which can be neglected.

The settling chamber is kept at sub-atmospheric conditions by the constant flow of air through the nozzle and the compressor. When, during surge, massflow through the compressor is reduced, the pressure increases towards a new equilibrium. Massflow during surge is unsteady and periodically reversing, but an average value can be calculated in a reference period Δt, starting from stall inception and lasting one or more cycles:

$$\dot{m}_{IN\ SURGE} = \int_0^{\Delta t} \dot{m}_{IN} dt / \Delta t \tag{5}$$

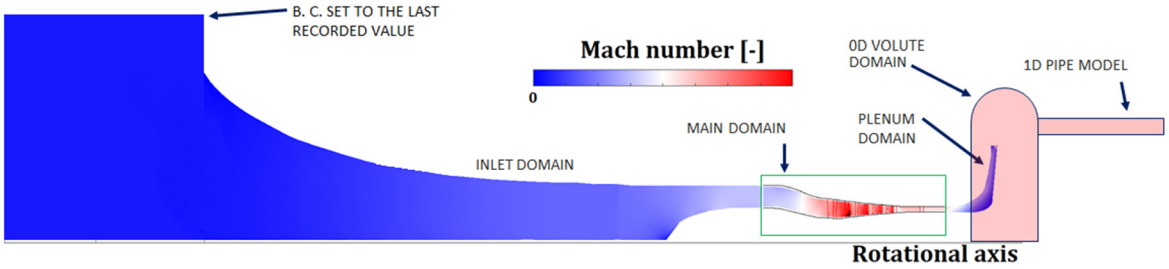

Fig. 5. Scheme of the model of Rig250 testbed in ACRoSS. Not in scale. (For interpretation of the colours in the figure(s), the reader is referred to the web version of this article.)

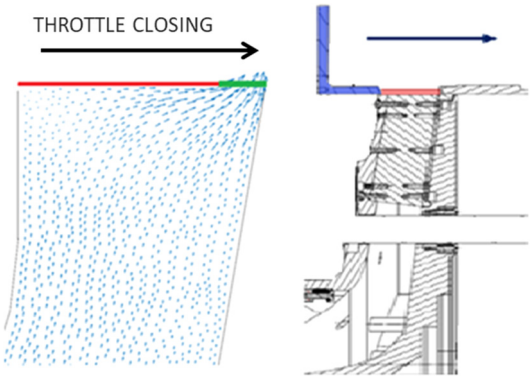

Fig. 6. Image of the plenum used in rig250 and the movement of its throttle (right) and the corresponding model in ACRoSS (left).

Assuming constant massflow through the inlet throttle, $\dot{m}_{CHAMBER\ IN}$, we can estimate the pressurisation in the chamber of volume V_{ST} during the period Δt

$$\Delta\rho = (\dot{m}_{CHAMBER\ IN} - \dot{m}_{IN\ SURGE}) \cdot \Delta t / V_{ST} \tag{6}$$

Using the results from ACRoSS we can estimate that, during surge, the density change in the settling chamber is $<0.5\%$ during a period Δt corresponding to the largest surge cycle investigated. The settling chamber is then assumed to have constant pressure and is not included in the model. A small portion of the chamber is included in the domain, to correctly capture the reflection of any wave emitted by the surge event, as in Fig. 5. The total pressure and temperature imposed as boundary conditions (BC) are constant and set to match the last steady measurement in the chamber before stall. All open domain boundaries use non-reflective boundary conditions and can handle both flow entering and exiting the domain. The bell mouth and the gas path around the spinner are introduced as a domain with a triangular mesh, with the method described in [19]; the singularity at $r = 0$ is avoided by setting a wall domain at $r = 0.01$ m. The struts in front of the compressor and at plenum inlet are not included. The main part of the domain contains all the blade rows; bleed valves and tip clearances are not included in the model.

The plenum is introduced as a 3D domain, rather than using a zero-dimensional model as it is common in low-order and lumped compressor stall models [10,13]. Due to its shape similar to a duct, especially in the minimum volume configuration, it is unrealistic to assume that all of the dynamic pressure is lost entering the volume, as is implied when using a 0D model. Including the full geometry also allows to correctly model any acoustic waves reflected in the plenum. The throttle is introduced using the method previously described, correctly reproducing the movement of its real-world counterpart, as shown in Fig. 6.

The exhaust system can be neglected with the assumption of the plenum throttle being always choked. This is achieved by setting the pressure at the outlet boundary to a constant low value, 50 kPa. However, a version of the model has been created which includes the volute/collector and the pipe connecting to the atmosphere, to take into account the inertia of the exhaust system, as shown in Fig. 5. The volute is modelled as an adiabatic 0D volume, assuming that all dynamic pressure of the flow through the plenum throttle is lost. The pipe is modelled using a 1-dimensional Euler solver, with the last recorded atmospheric pressure as boundary condition at the far outlet.

While ACRoSS is designed to simulate compressor stall in 3D, the results suggest that in both cases investigated the three-dimensional effects are insignificant, and no macroscopic difference exists in performance between 3D and 2D (axi-symmetric) simulations, Fig. 7. The three-dimensional effects include the presence of transient rotating stall, which is observed during flow reversal and recovery in the 3D simulation. This finding indicates that a 2D simulation could be sufficient to model the bulk of the performance during deep surge in a single compressor, as was also previously observed in a high-speed IPC modelled by Righi et al. [19]. However, when shaft speed and plenum volume are modified, the stall event can change continuously from 'deep' to 'mild' surge, to rotating stall. It is unknown at which point along this evolution the 3D features become relevant for a certain compressor, although clearly 2D simulations are never appropriate for rotating stall. Therefore, when simulating a new compressor or new operating condition the validity of 2D simulations should be confirmed by comparison with a 3D full annulus simulation, at least for the surge event with the highest frequency.

Having confirmed their validity for the current application, 2D simulations are used reducing by 2 orders of magnitude the computational cost. The mesh used for the simulation has 1800 axial and 7 radial elements, the inlet domain has $\sim$12000 elements and the plenum has $\sim$15000 elements. A grid convergence study is performed following the method described by Celik and Karatekin [28], and the grid selected is found to have a $< 5\%$ error from the extrapolated grid independent value of massflow, pressure ratio and temperature ratio. The overall domain of 39000 elements requires $\sim$1 hour of computation for 130 revolutions using 40 Intel Xeon 2.1 GHz CPUs; the 3D simulation (with 90 circumferential elements) would instead require $\sim$1 day per 30 revolutions with the same computational power.

In both simulations the shaft speed is constant, no bleed valves, variable geometries or tip clearances are included. The absence of tip clearance modelling makes the prediction of the stall inception and of the surge line position less accurate. However, as it was observed in previous validations and in the current work, this does not substantially affect the matching of the overall surge event [19].

A single simulation is first run with sequential throttling steps to create the unstalled characteristic; the simulation is then restarted at the last operating point before the surge line and the throttle is close by 2%, to trigger the stall. During surge the throttle is kept constant.

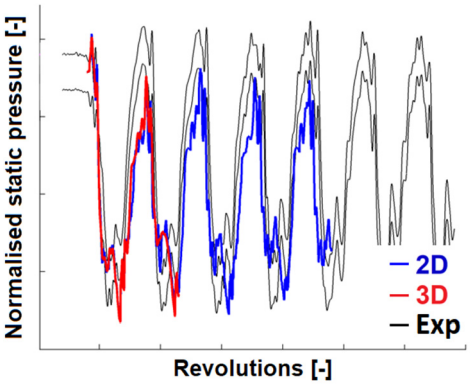

Fig. 7. Comparison of static pressure at rotor 1 inlet casing modelled using the 2D (axis-symmetric) and 3D versions of ACRoSS. Two experimental measurements are included for reference.

4. Results and discussion

4.1. Steady simulation

To assess the accuracy of the empirical correlations for unstalled forward flow, the design speed characteristics are reproduced and compared with what was recorded experimentally, as shown in Fig. 8. Simulated part-speed characteristics are also presented, although the corresponding experimental data is not available for comparison. Characteristics are run from choking conditions, below which corrected massflow and temperature ratio remain constant, to the surge line. The last operating point on the characteristic is investigated by closing the throttle with 1% increments until stall occurs.

For the 100% NRT speed-line, the corrected massflow at design point and at the surge line is matched within 4%, while the maximum pressure and temperature rise before surge are matched within 3%. Additionally, for the last operating point on the characteristic before stall, the total pressure at each stator LE is compared with values measured locally by probes, matching with less than 5% error. The ACRoSS simulation overestimates the corrected massflow along the 100% NRT characteristic, especially close to choking. This is in part attributed to the fact that the model does not include blade metal or aerodynamic blockage, and the flow can always occupy the full annulus section.

This level of deviation from experimental performance is deemed acceptable for the purposes of this study and the fidelity of the code, no calibration or tuning of the empirical correlation is performed.

4.2. Case 1 – minimum volume

Surge is simulated in ACRoSS using the choked nozzle assumption and the results are shown in Fig. 9, comparing the static pressure measured by unsteady pressure probes and virtual probes at each rotor inlet on the tip. The experimental and numerical measurements are non-dimensionalised using the last recorded steady value of static pressure at the same position. The period of each surge cycle is calculated by measuring the time between some relevant feature: for rotors 1-3 the peaks caused by the surge pressure wave peaks are used, for rotor 4 the pressure drop at the beginning of each cycle. The characteristic shape of the pressure profiles at each stage is correctly reproduced by ACRoSS, and the average period is matched within 5% for 5 cycles. The simulated profiles show realistic magnitude in all stages, although due to uncertainty in the measurement it is not possible to quantify this.

While the results agree closely with the experimental data, the assumption is made of constant 50 kPa at the outlet to maintain the nozzle choked. However, as in reality this is connected to the atmosphere with a pipe, this is highly unrealistic. If the ACRoSS simulation is run with the plenum discharging directly to atmospheric conditions, the flow reverses into the plenum during surge and the surge period increases by 300%, eventually developing into a rotating stall.

If the whole exhaust system including the pipe is modelled, when during surge the massflow in the throttle reduces, the volute will de-pressurise accordingly, as can be observed in Fig. 10. This ensures that the plenum keeps discharging during the cycle and the correct period is obtained; the comparison with measurements is presented in Fig. 11. These results indicate that the specific exhaust system of the facility plays a role in determining the post-stall behaviour.

The expansion wave which is produced when the volute depressurises travels through the pipe and is reflected by the outlet to the atmosphere. The reflected wave re-pressurises the volute, approximately 40 revolutions after the compressor stalls, causing the next surge event to be completely different from the others. This is a clear diversion from the experimental data, in which surge cycles are constant in shape and size for several instances (see Fig. 11), for this reason, the results from this model are discarded after the first 2 cycles. The divergence is likely to be caused by the simple modelling of the volute as 0D and the pipe as a 1D, constant-area, straight domain. The real piping has variable area and turns which gradually reflect the outgoing wave, whereas the 1D model maximises the magnitude of the reflected wave. The real volute will recover part of the entering dynamic pressure at lower massflow, which helps maintaining the flow in the pipe; the 0D volute instead is assumed to always dissipate all the dynamic pressure. Since the geometry of the exhaust ducting and volute is not available and their unsteady flow was not measured, it is impossible to create or validate a more appropriate model.

4.3. Case 2 – maximum volume

When the maximum volume case is modelled using ACRoSS, a very characteristic behaviour is observed, as shown in Fig. 12.

Two simulations are run for the same case, with the performance of the compressor modelled slightly differently. This can be obtained for example by a small change in the empirical correlations tuning or the body force stiffness; in Fig. 12 the difference is a 50% change in the body force stiffness (K constant in Eq. (3)). The simulations have minimal difference during reversal and recovery but during re-pressurisation, while the compressor is unstalled, simulation B re-enters stall while simulation A continues until maximum pressure rise is reached, resulting in a period ∼33% longer. The origin of the second stall inception is located in stage 4, its pressure rise during the surge cycle is shown in Fig. 12b. Even though the overall compressor re-pressurisation phase lasts from revolutions ∼35 to 46, during this period the last stage is operating very close to its maximum pressure rise (similar to the pre-stall value). In this phase, a small change in performance is sufficient to cause stage 4 in simulation B to go beyond its surge line and re-enter stall earlier at rev. 36.

When various changes in performance are tried, the variation in surge period is not continuous but always results within 2-3% of one of the two simulations shown in Fig. 12. The two different periods occur even within a single simulation with constant parameters, as shown in Fig. 13; in the same simulation one surge has a longer period, (as in simulation A), while the other 4 have a very similar smaller period, (as in simulation B). This indicates that even though the operation close to the surge line lasts for over 10 revolutions, there is a particular event occurring ∼ 30-32 revolutions after surge began, which can trigger a new stall. A second event, occurring after 20-22 revolutions can also be observed in-

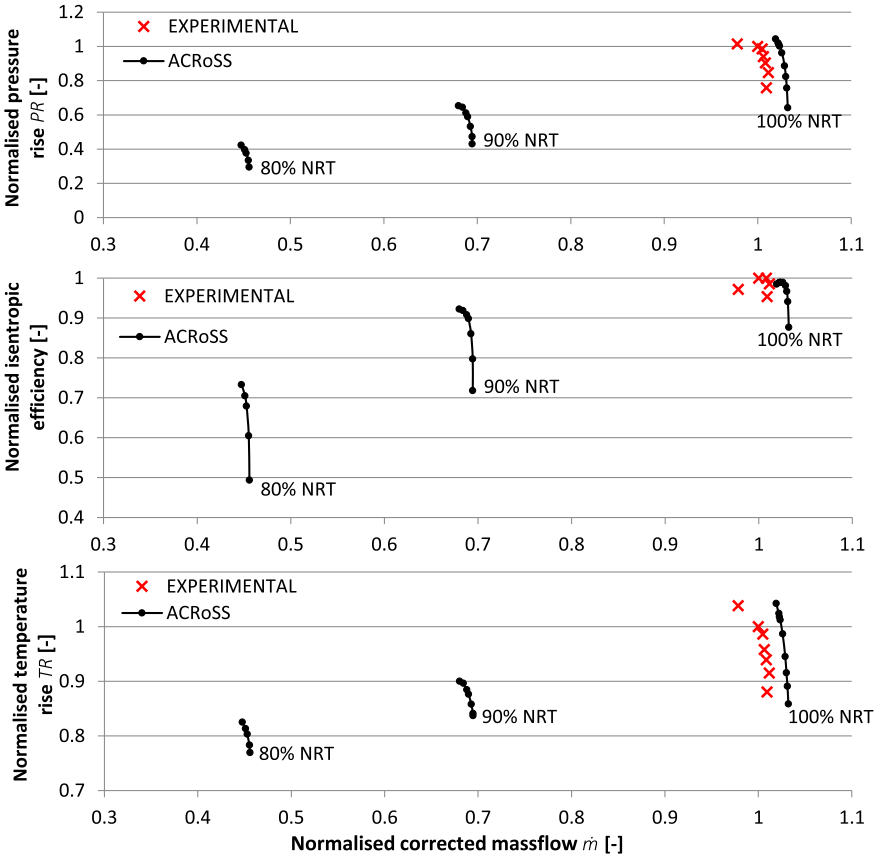

Fig. 8. Comparison of the unstalled characteristic, experimentally measured and simulated.

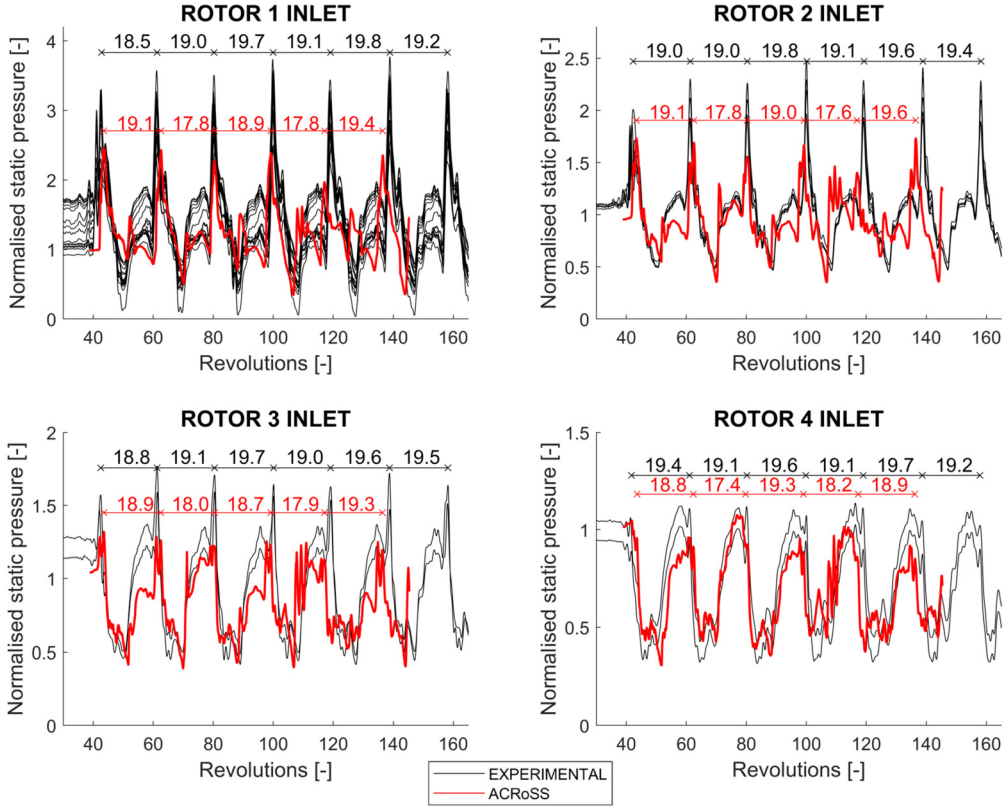

Fig. 9. Static pressure at each rotor inlet tip, comparison of experimental data and ACRoSS simulations, with choked nozzle. Case 1 minimum volume.

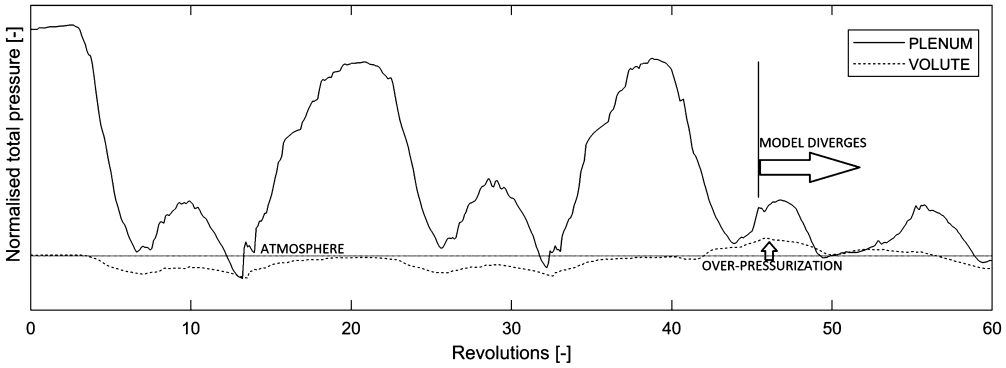

Fig. 10. Evolution of pressure in the plenum and in the volute during surge, with the exhaust system modelled.

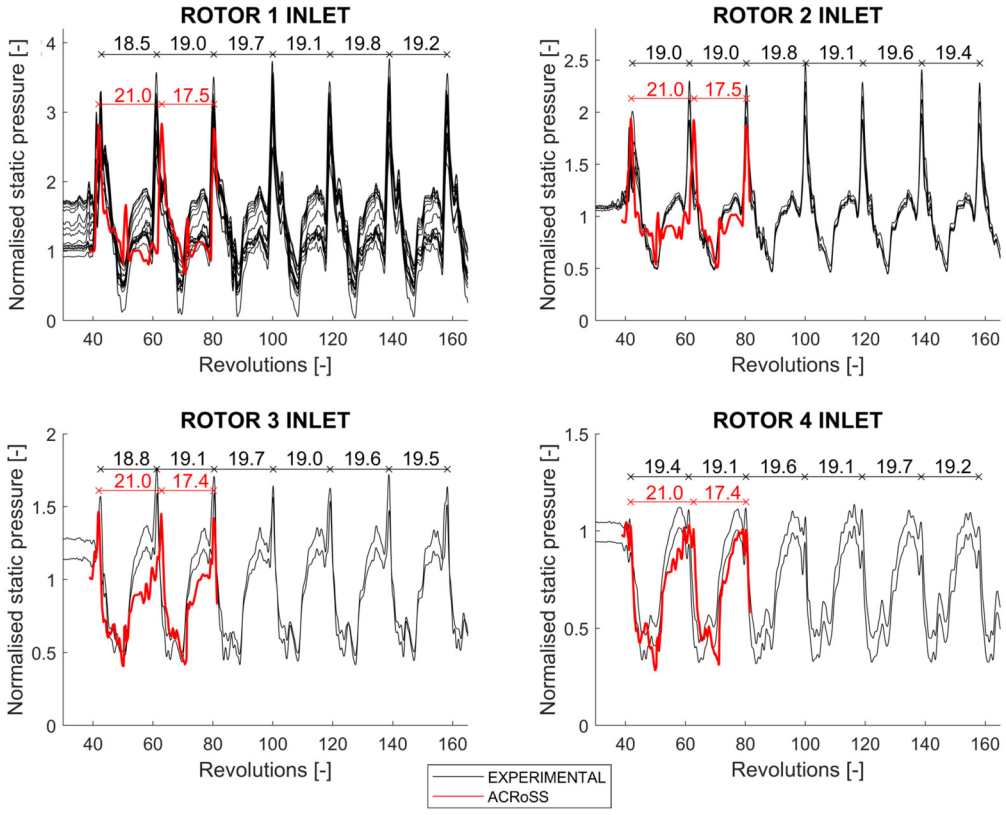

Fig. 11. Static pressure at each rotor inlet tip, comparison of experimental data and ACRoSS simulations, with exhaust pipe model. Case 1 minimum volume.

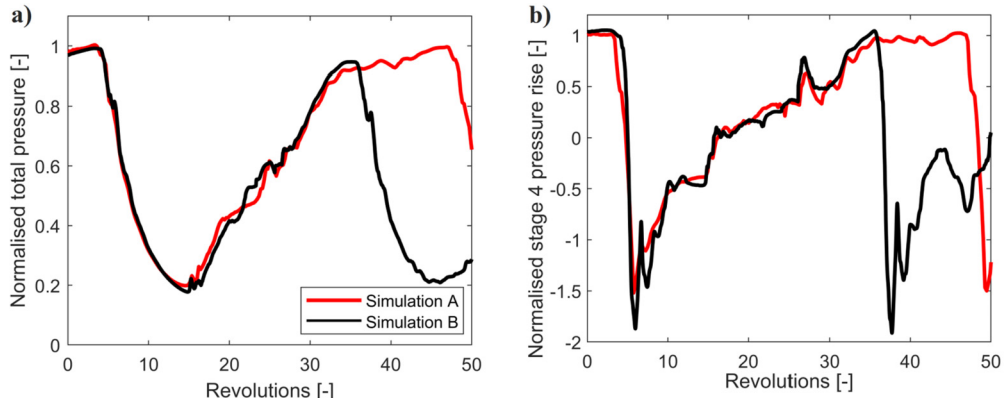

Fig. 12. Comparison of pressure in the plenum (a) and stage 4 pressure rise (b) for maximum volume case, between two ACRoSS simulations with a small variation in performance.

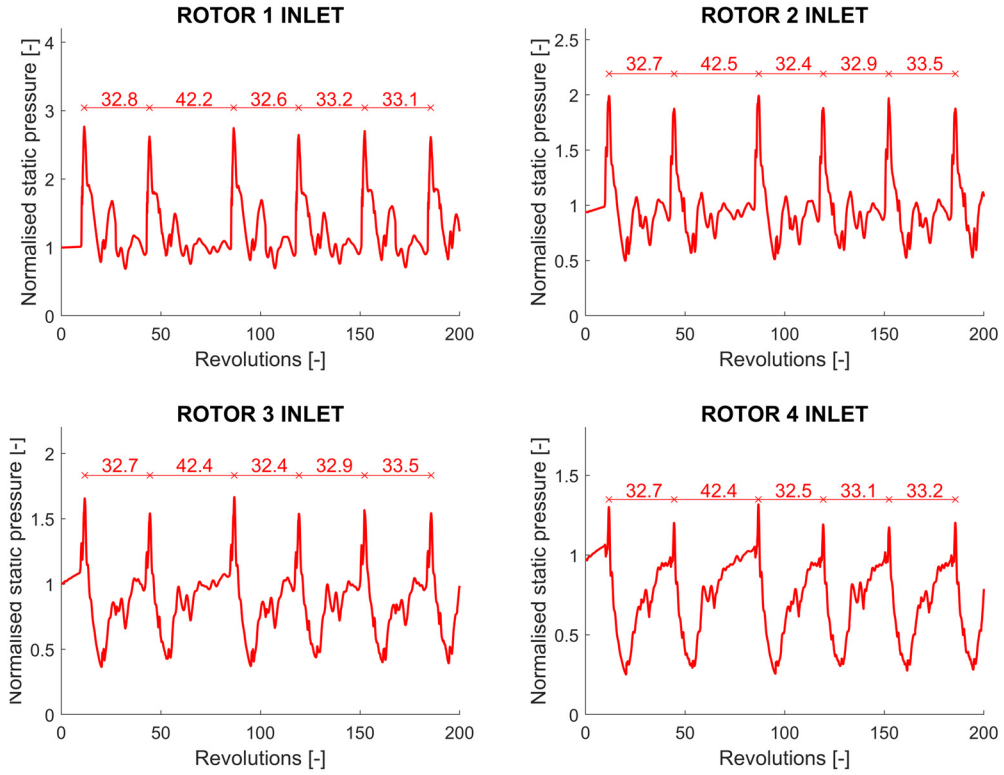

Fig. 13. Static pressure at each rotor inlet tip from ACRoSS simulation, with choked nozzle. Case 2 maximum volume.

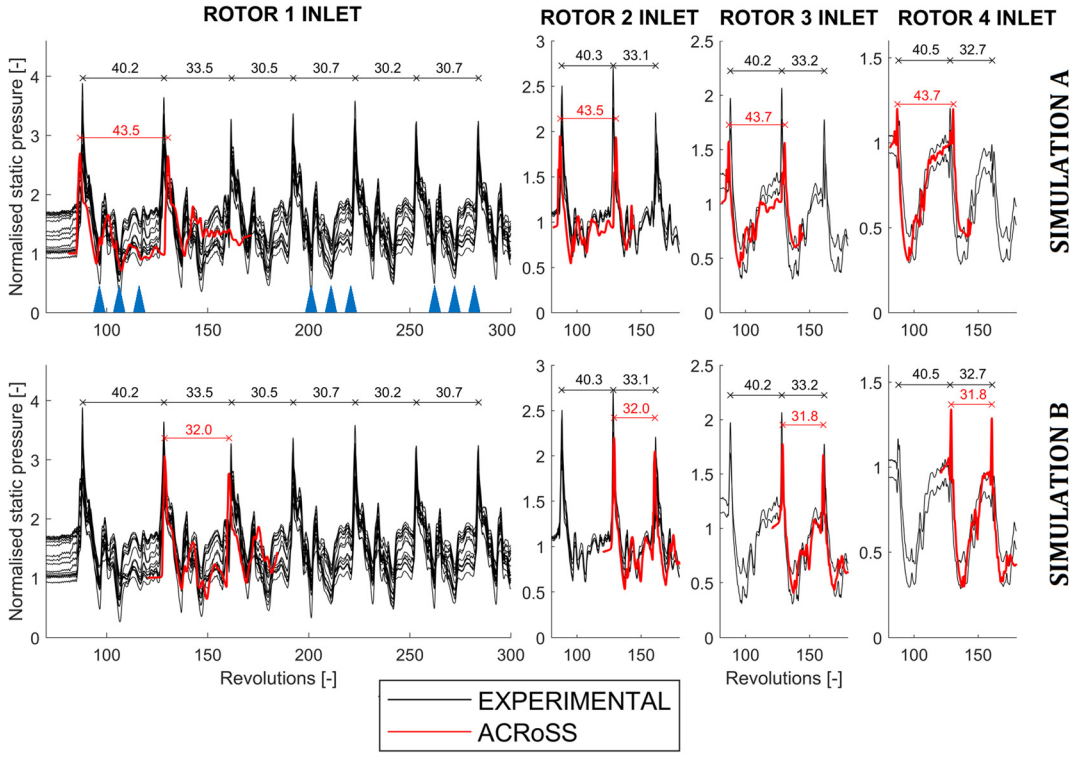

Fig. 14. Static pressure at rotors inlet, comparison of experimental data and simulations A and B from ACRoSS, with exhaust pipe model. Case 2 maximum volume.

creasing the local pressure rise in both simulations. The nature of these events this will be further discussed in Section 4.4.

Simulations A and B, obtained using the model with the exhaust system, are compared with the experimental measurements, as shown in Fig. 14. Even though the experimental rig was decelerating during case 2, all ACRoSS simulations are run with constant speed. The profiles are non-dimensionalised in time using the rotational speed before the deceleration start; therefore, as the rig slows down the period indicated remains a measure of time and *not* of the number of revolutions. The traces from the unsteady pressure transducers highlight that two specific periods exist for the surge cycle, similar to what was observed in ACRoSS. The re-

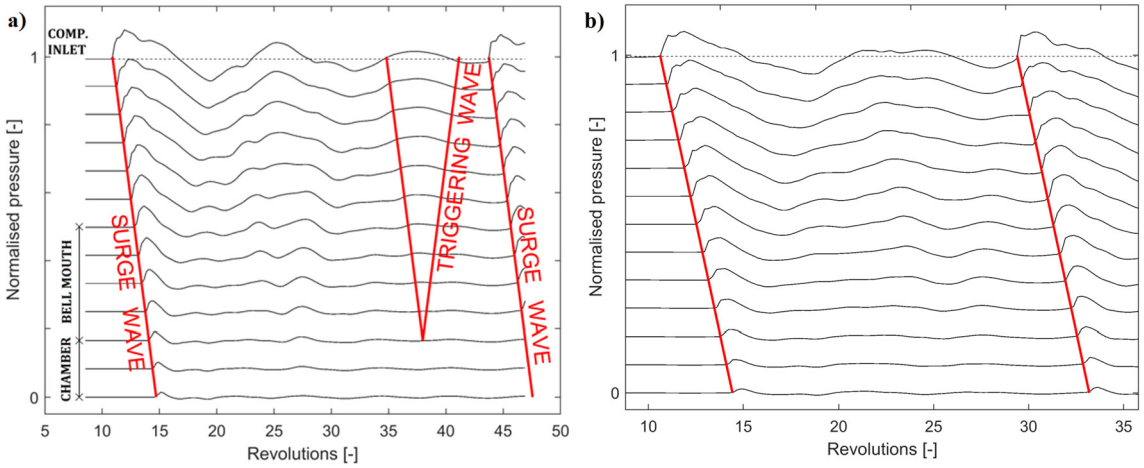

Fig. 15. Analysis of static pressure at different positions along the inlet duct modelled by ACRoSS. The surge wave and the wave triggering the stall are highlighted. Case 2 simulation B (left), Case 1 (right).

sults from the model are then compared by aligning simulation A with the longer cycle and simulation B with the shorter. ACRoSS is found to reproduce very closely the specific shapes of the pressure traces, with the surge periods matched within 10%. For both simulations the magnitude of the pressure oscillations has a similar range to the measured values.

In Case 2 the compressor stall is triggered by an emergency shutdown of one of the motors and the compressor decelerates during the event, with a reduction of about 12% RPM obtained in the time considered. It is reasonable to assume that the compressor performance reduces continuously with speed, but the surge cycles observed switch directly from one period to the other and remain constant for the last four. These results indicate that while surge frequency depends on the performance, it does not vary continuously with it, changing instead between two possible outcomes. This is similar to what is observed in ACRoSS, suggesting the presence in the experiment of the same event occurring ∼30 revolutions after stall inception which controls the period of the shorter surge cycles.

It is not certain if in the experimental rig the first surge cycle is always longer than the others, as a case with decelerating shaft did not occur again in the campaign. The authors propose as an explanation that, as it was modelled in ACRoSS, the last stage of the experimental rig is operating close to its surge line. The event observed ∼30 revolutions after the beginning of the cycle does not trigger a new surge the first time, when the compressor is running at full speed. However, as the rotational speed decreases the compressor performance and surge margin reduces and, in all subsequent cycles, this event always causes a new stall.

It should be noted that in the experimental data the change in performance is due to the decelerating compressor while in ACRoSS it is caused artificially by modifying the parameters of the body force models. Despite this, the physical behaviour through which the change in performance affects the surge period remains the same. In particular, ACRoSS correctly simulates the 4^{th} stage operating close to its surge line during re-pressurisation, and correctly predicts the event that causes the local pressure rise increase at a specific time during surge. The accurate modelling of the performance of each stage is therefore critical to reproduce the surge behaviour of Rig250; this event could not be reproduced by lumped models using overall compressor characteristics.

4.4. Interference with inlet duct

Highlighted in Fig. 14 are a set of peaks of low pressure which occur in every cycle with the same timing at rotor 1 inlet, these are observed both in experimental measurements and in the ACRoSS simulations. In the first cycle the third drop occurs during re-pressurisation without any consequence, but in the later cycles it is always immediately followed by a pressure peak caused by the new stall. The 2^{nd} and 3^{rd} pressure drops coincide with the two events observed in ACRoSS in Fig. 12. As seen in the pressure traces of Case 2 (maximum volume), presented in Fig. 15a, these peaks are caused by the pressure at compressor inlet oscillating three times around the value in the settling chamber, down to a ∼60 kPa de-pressurisation with respect to the atmosphere. The pressure in the settling chamber (at 0 in the figure) remains constant due to its large volume, whereas the choked plenum can change its pressure freely. As a result, the pressure of the whole compression system oscillates together with the value at inlet. Observing the pressure evolution in the bell mouth, we can identify an expansion wave moving towards the compressor just before stall occurs. When an expansion wave travels downstream through the compressor it increases locally the load, causing the two events in the 4^{th} stage.

The pressure oscillations at compressor inlet are driven by the reflections of the first surge wave emitted. Although there are multiple changes in the inlet cross-sectional area, causing overlapping reflections, the timing appears to be controlled by the duct length, with the 3^{rd} peak of low pressure occurring always ∼30 revs after the initial surge wave.

The same investigation is also performed on Case 1 (with the minimum volume), and the pressure in the inlet duct is shown in Fig. 15b. In this case, we can observe that the pressure at compressor inlet is again oscillating around the value in the settling chamber, with the next stall inception occurring when the 2^{nd} expansion wave reaches the compressor. Therefore, while the smaller plenum volume influences the surge cycle making it shorter than Case 2, the exact period is very likely to be determined by the inlet duct length. The new stall is triggered by the 2^{nd} wave, instead of the 3^{rd}, making the period shorter than Case 2. This hypothesis is further supported by the fact that the pressure rise in Case 1 does not return to the maximum value in every cycle, but the recovery is interrupted by the next stall inception, as can be seen in the rotor 4 measurement in Fig. 9.

In both cases the initial surge wave instantly reverses the flow in the inlet duct up until the inlet boundary, however the hot gas generated by the blades in reverse flow remains confined in the inlet duct and is convected downstream when recovery occurs. All of the hot gas is expelled through the plenum nozzle before the start of the next surge cycle.

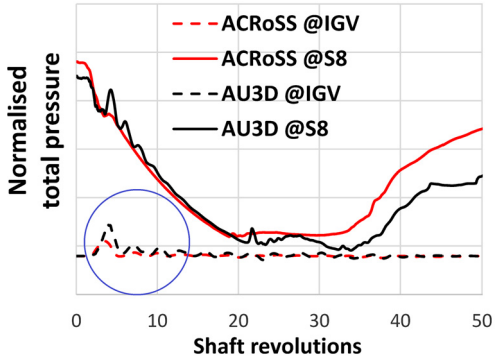

Fig. 16. Traces of pressure at compressor inlet (@IGV) and outlet (at stator 8, S8) during a surge event, with the pressure oscillation at inlet highlighted, data from Righi et al. [14].

ACRoSS was previously used to model surge on a different geometry, presented in Righi et al. [14], Fig. 16. In that article, the simulation form ACRoSS was compared and successfully validated with high-fidelity URANS 3D simulations, performed at Imperial College London using the code AU3D Zhao et al. [7]. In that case the opening in the inlet duct was less than a compressor length away from the IGV, and the initial surge wave was reflected more than 5 times in the inlet before recovery occurred. As a result, the inlet pressure was practically constant during recovery and re-pressurisation, and could not affect the surge. The long, mostly straight duct used in Rig250 instead, causes the inlet pressure to oscillate slowly and with large magnitude, interfering with the surge cycle and locking it into a specific period which is a function of inlet geometry.

To further verify this conclusion, Case 2 is run again using a 50% shorter duct, constant speed and choked nozzle. During the first 30 revolutions after surge begins, 6 pressure oscillations can be observed at the inlet (double compared to the case with the original duct). As a result, the oscillations are dampened before the re-pressurisation phase of the cycle and, without any triggering wave, the compressor always returns to the maximum pressure rise before the next stall. All 5 cycles simulated lasted around 39 revolutions, similar to Case 2 Simulation A. This suggests that the surge behaviour can be made independent from the inlet duct by reducing its length.

The correct modelling of the surge wave reflection is a capability critical for the modelling of the post-stall behaviour of Rig250. To obtain this level of simulation matching in ACRoSS, the inlet duct and the transition into the settling chamber had to be included in the domain, see Fig. 5. Simpler lumped models, or any model not considering the ducting geometry, would be unable to correctly reproduce the dependency of the surge period form the wave reflections.

5. Conclusions

The unsteady through-flow code ACRoSS has been validated using unsteady pressure measurements of two surge events from a high-speed experimental rig, demonstrating the applicability of this low-order model to commercially relevant aero-compressors. A close matching is obtained for both cases in the shape and period of the pressure traces at each stage. Two-dimensional, axisymmetric simulations are found to be sufficient for the cases investigated, and the code can provide accurate surge simulation with a computational cost of less than an hour per event on 40 CPUs.

The validation of the ACRoSS model has allowed to investigate the effect that the testbed ducting has on the post-stall behaviour. To correctly reproduce the surge event, the inlet bell mouth, the plenum, and the exhaust piping connecting to the atmosphere had to be included in the model.

An unusual behaviour was observed in the surge frequency for the maximum volume case, both in the simulation and in the experimental data; this was investigated using the unsteady model. In this surge event the compressor decelerates in time but, after a first longer cycle, all the subsequent surges have a constant shorter period. The results indicate that the long ducting in front of the compressor causes the pressure of the whole system to oscillate around the value in the settling chamber. This oscillation increases periodically the compressor loading, with timing controlled by the inlet duct length and geometry, causing stall to be the triggered always at a specific moment in time. In the maximum volume case, stall is triggered at the third oscillation, in the minimum volume case this occurs at the second.

These findings highlight the importance, when testing surge experimentally or numerically, of carefully selecting the geometry and distance between the compressor and the settling chamber (or atmosphere) to be representative of the real geometry of interest. The handling of the exhaust from the compressor can also heavily influence the post-stall behaviour, especially if a sub-atmospheric inlet pressure is used.

Declaration of competing interest

The authors declare that they have no known competing financial interests or personal relationships that could have appeared to influence the work reported in this paper.

Acknowledgements

The authors would like to express their gratitude to Rolls-Royce plc. for funding this research and for permission to publish this paper. Special thanks to Mr. Richard Tunstall and Mr. Arthur Rowe from Rolls-Royce plc. for supervising this work. The presented test data set was generated within the research project EcoFlex (FKZ: 03ET7091H), which is funded by the German Federal Ministry of Economics and Technology. The authors gratefully acknowledge Rolls-Royce Deutschland Ltd & Co KG and the DLR Institute of Propulsion Technology for granting permission for its publication, their support and for providing the rig test measurement data.

References

[1] W. Hosny, W. Steenken, Aerodynamic instability performance of an advanced high-pressure-ratio compression component, in: AAIA/SME/SAE/ASEE 22nd Joint Propulsion Conference, Huntsville, AL, June 16-18, 1986.
[2] J. Dodds, M. Vahdati, Rotating stall observation in a high speed compressor - part I: experimental study, J. Turbomach. 137 (5) (2015), https://doi.org/10.1115/1.4028557.
[3] T. Giersch, F. Figaschewsky, P. Hönisch, A. Kühhorn, S. Schrape, Numerical analysis and validation of the rotor blade vibration response induced by high pressure compressor deep surge, in: ASME Turbo Expo 2014: Turbine Technical Conference and Exposition, Düsseldorf, Germany, June 16–20, 2014, ASME Paper No. GT2014-26295.
[4] M. Zhu, J. Teng, X. Qiang, Unsteady near-stall flow mechanisms in a transonic compressor rotor at different rotating speeds, Aerosp. Sci. Technol. 119 (2021), https://doi.org/10.1016/j.ast.2021.107124.
[5] M.P. Manas, A.M. Pradeep, Stall inception in a contra-rotating fan under radially distorted inflows, Aerosp. Sci. Technol. 105 (2020), https://doi.org/10.1016/j.ast.2020.105909.
[6] T. Giersch, Numerical Models for the Vibration Response of High Pressure Compressor Rotors with Validation for Forced Response and Surge, PhD Thesis, Brandenburg University of Technology, Germany, 2018.
[7] F. Zhao, J. Dodds, M. Vahdati, Flow physics during surge and recovery of a multi-stage high-speed compressor, J. Turbomach. 143 (6) (2020), https://doi.org/10.1115/1.4050240.
[8] J. Moreno, J. Dodds, C. Sheaf, F. Zhao, M. Vahdati, Aerodynamic loading considerations of three-shaft engine compression system during surge, in: ASME Turbo Expo 2020: Turbomachinery Technical Conference and Exposition, Virtual Conference, 2020. Online, ASME Paper No: GT2020-14305.

[9] M. Haake, R. Fiola, S. Staudacher, Multistage compressor and turbine modelling for the prediction of the maximum turbine speed resulting from shaft breakage, J. Turbomach. 133 (2) (2011) 1–12, https://doi.org/10.1115/1.4001188.
[10] E.M. Greitzer, Surge and rotating stall in axial flow compressors part I: theoretical compression system model, J. Eng. Power 98 (1976) 190–198, https://doi.org/10.1115/1.3446138.
[11] Y. Gong, A Computational Model for Rotating Stall and Inlet Distortions in Multi-stage Compressors, PhD Thesis, Massachusetts Institute of Technology, Massachusetts, 1999.
[12] M.L. Brand, An Improved Blade Passage Model for Estimating Off-Design Axial Compressor Performance, MSc Thesis, Massachusetts Institute of Technology, Massachusetts, 2013.
[13] J.P. Longley, Calculating stall and surge transients, in: Proceedings of the ASME Turbo Expo 2007: Power for Land, Sea, and Air, Montreal, Canada, May 14–17, 2007, pp. 125–136, ASME Paper No: GT2007-27378.
[14] S. Rosa Taddei, A novel blade force approach to two-dimensional meanline simulation of transonic compressor rotating stall, Aerosp. Sci. Technol. 111 (2021), https://doi.org/10.1016/j.ast.2021.106509.
[15] J. Guo, J. Hu, X. Wang, R. Xu, A three-dimensional unsteady through-flow model for rotating stall in axial compressors, in: Proceedings of the ASME Turbo Expo 2020: Turbomachinery Technical Conference and Exposition, ASME, 2020. Virtual, Online. September 21–25, 2020.
[16] H. Zeng, X. Zheng, M. Vahdati, A method of stall and surge prediction in axial compressors based on three-dimensional body-force model, J. Eng. Gas Turbines Power 144 (3) (2022).
[17] M. Righi, V. Pachidis, L. Könözsy, On the prediction of the reverse flow and rotating stall characteristics of high-speed axial compressors using a three-dimensional through-flow code, Aerosp. Sci. Technol. 99 (2020), https://doi.org/10.1016/j.ast.2019.105578.
[18] M. Righi, V. Pachidis, L. Konozsy, L. Pawsey, Three-dimensional through-flow modelling of axial flow compressor rotating stall and surge, Aerosp. Sci. Technol. 78 (2018) 271–279, https://doi.org/10.1016/j.ast.2018.04.021.
[19] M. Righi, V. Pachidis, L. Könözsy, F. Zhao, M. Vahdati, Three-dimensional low-order surge model for high-speed axial compressors, J. Glob. Power Propuls. Soc. 4 (2020) 274–284, https://doi.org/10.33737/jgpps/130790.
[20] F. Figaschewsky, A. Kühhorn, A. Beirow, T. Giersch, S. Schrape, Analysis of mistuned forced response in an axial high pressure compressor rig with focus on Tyler-Sofrin modes, Aeronaut. J. 123 (1261) (2017) 356–377, https://doi.org/10.1017/aer.2018.163.
[21] F. Franz, A. Kühhorn, T. Giersch, S. Schrape, F. Figaschewsky, Influence of inlet distortions on the forced vibration of a high pressure compressor rig, in: ASME 2020 Turbo Expo - Virtual Conference Session Gallery, 2020. ASME Paper No: GT2020-16221, Virtual Conference, Online, September 21-25.
[22] O. Reutter, G. Ashcroft, E. Nicke, E. Kügeler, Unsteady full annulus multi-stage compressor calculations-details on cfd-experiment comparison, in: 4th AIAA/CEAS Aeroacoustics Conference, Bucharest, Romania, October 16-20, 2017.
[23] O. Reutter, G. Ashcroft, E. Nicke, E. Kuegeler, Comparison of experiments, full-annulus calculations and harmonic-balance-calculations of a multi-stage compressor, in: Proceedings of Montreal 2018 Global Power and Propulsion Forum, Montreal, Canada, May 7-9, 2018.
[24] O. Reutter, E. Gerd, D. Theo, P. Andreas, Experimental investigation of inlet distortion in a 4.5-stage axial compressor, in: ASME Turbo Expo 2020: Turbomachinery Technical Conference and Exposition, 2020. Virtual Conference, Online, September 21-25, ASME Paper No GT2020-16201.
[25] L. Meillard, R. Schnell, E. Nicke, M. Voges, C. Voigt, Verification of the three dimensional shock-structures in an s-shaped transonic UHBR fan-rotor, in: 11th European Turbomachinery Conference, Madrid, Spain, March 23-27, 2015.
[26] D. Schönweitz, M. Voges, G. Goinis, G. Enders, E. Johann, Experimental and numerical examinations of a transonic compressor-stage with casing treatment, in: ASME Turbo Expo 2013: Turbine Technical Conference and Exposition, San Antonio, Texas, June 3–7, 2013.
[27] H.L. Moses, S.B. Thomason, Approximation for fully stalled cascades, J. Propuls. Power 2 (2) (1986) 188–189.
[28] I. Celik, O. Karatekin, Numerical experiments on application of Richardson extrapolation with nonuniform grids, J. Fluids Eng. 119 (3) (1997) 584–590.

Experimental validation of a three-dimensional through-flow model for high-speed compressor surge

Righi, Mauro

2022-08-09

Righi M, Pachidis V, Könözsy L, et al., (2022) Experimental validation of a three-dimensional through-flow model for high-speed compressor surge. Aerospace Science and Technology, Volume 128, September 2022, Article number 107775

https://doi.org/10.1016/j.ast.2022.107775